

A mixture of Noise Image Denoising using Sevenlets Wavelet Techniques

Beera Babu Srinivas Kumar^{1,*} and Periyapattinam Srinivasaiah Satyanarayana²

¹Jain University, K.L.E.Society's C.B.Kolli Polytechnic, Haveri, India

²Department of Electronics and Communication Engineering, BMS College of Engineering, Bangalore, India

(*Corresponding author's email: bbskumarindia@gmail.com)

Received: 12 December 2020, Revised: 26 May 2021, Accepted: 12 June 2021

Abstract

The noise has always been present in digital images when coding, image acquisition, transmission and processing steps has often corrupted by noise. Noise is challenging to confiscate from the digital images without the noise model's prior information preserving edges. That is why the assessment of noise models is essential in the revise of image denoising techniques. A novel approach to improve the performance of an image's quality and visual perception must be noise-free. The essential features like edge details should be retained as much as possible due to the increased traffic caused by multimedia information and digitized form of representation of images. This research articulates a brief general fundamental proposal of the noise model. The input image has debased with different noise probability density of Gaussian (G), Speckle (S), Salt and Pepper (SP) noise and a mixture of noise (G + S + SP). The Wavelet technique's methodology using Sevenlets wavelet are Haar, Daubechies, Coiflets, Symlets, Discrete Meyer, Biorthogonal and Reverse Biorthogonal input Lena standard image has decomposed using Discrete Wavelet Transform (DWT). The decomposition process, as accomplished by discriminating the input image with lower and higher image coefficients. Filtering techniques are employed to deplete the noise present in an image. Hence the quantitative investigation of noise model at hard and soft thresholding is analyzed, improving image quality by increasing PSNR and decreasing MSE to have better performance.

Keywords: Discrete wavelet transform, Denoising, Peak signal to noise ratio, Mean square error

Introduction

Image denoising is a concern in numerous computer vision and denoised image processing challenges [1]. Different existing techniques for image denoising as researched. A successful system's key feature that denoising image is to remove noise much further than necessary and preserve boundaries and the information necessary to preserve images by improving visual quality. This inquisition presents some vital work in denoising images categorized as spatial domain methods, transform domain methods, or integrate to obtain their advantages. This work attempted to concentrate on this composition between wavelet transform and spatial domain filters. Various algorithms were published, and each methodology has its principles, strengths and constraints according to different advantages and noise. In their techniques, assessment explore would have performed compared to obtain denoising algorithms, wavelet-based and filter methods. Standard measurement parameters would be used in specific analysis to examine techniques, and with the addition of evaluation metrics, some other methods as used to analyze denoising strategies. The main objective is to process simultaneously for 7 wavelets at a time to find the analysis when the mixture of noise as added to the image before applying wavelet transform and spatial domain linear (Wiener) and non-linear (Median) filters, noise and blurring removal and clarity of image quality main criteria of this analysis denoising processing. At soft and hard thresholding levels it is investigated to obtain better image quality when corrupted with noise density particularly G, S and SP. Noise is a part of during transmission processing externally and internally it is very significant visualization image noise free to understand for analysis at every sector of discovery field.

The 7 wavelets would have used hence called by new term Sevenlets Wavelet is used for this investigation work to analyze a Lena standard image of 2-dimensional JPEG (Joint Photographic Experts Group) format, simulation carried out using Matlab. It is very significant in image processing techniques to retrieve the image for any network processing breakthrough to perfection with efficiency in the digital image processing field. Wavelets have used Haar, Daubechies, Symlets, Coiflets, Discrete Meyer, Biorthogonal and Reverse Biorthogonal waveforms representation having a short name with order haar, db2, sym4, coif2, dmey, bior6.8 and rbio6.8 have used for this experimental analysis.

Materials and methods

Various techniques based on wavelet transform with some spatial domain filters such as Wiener and Median filters are employed to preserve the image’s details and edges as much as possible. Therefore, this exploration presents a classical image denoising approach of various 7 wavelet methodologies adopted to obtain the optimum image denoising performance. The survey of different types of methods shows that some of them depended on using the primary DWT. Some of them depending on complex WT (Wavelet Transform) using filters to remove single or mixed type (multiplicative) of noise such as G, SP and S in the noisy image to obtain denoising image that to be close to the original image as much as possible depending on various threshold techniques like soft thresholding, hard thresholding, and measurement parameters have used to evaluate methods. These various methods still lag in the image’s better visual quality, so additional performance would have calculated to study the different wavelet techniques’ behavior by not compromising various noise reduction fields. A better technique with a suitable filter model designed to remove single and mixed noise in images in all areas gives a better visual appearance without destitution of the image’s details and considers the denoising image’s processing time.

Wavelet analysis

Analysis of a non-stationary signal using either the FT (Fourier Transform) or the STFT (Short Time Fourier Transform) does not result satisfactorily. Using wavelet analysis may have obtained better results. One advantage of analyzing wavelets is its ability to perform local analysis. Analysis of wavelets may reveal signals that other analytical techniques overlook, such as trends, breakdown points, discontinuities, etc. Especially in comparison with the STFT, wavelet analysis allows a multiresolution analysis to have performed.

Multiresolution analysis

The problem of time (t)-frequency (f) resolution would have caused the Heisenberg principle of uncertainty and exists regardless of the technique used for the analysis. For the STFT, a fixed resolution of the time-frequency would have used. When using a method called the Multiresolution Analysis (MRA), a signal can have analyzed with various resolutions at different frequencies. The Resolution Shift is displayed schematically, as seen in **Figure 1**. For resolution, as expected, low frequencies remain for the whole length of the signal, while high frequencies behave as a brief burst from time to time. For functional implementations, this is also the case. Analysis of the wavelet measures the correlation between the given signal and a wavelet function $\psi(t)$. For various periods, the resemblance between the signal and the evaluating wavelet function has calculated independently, resulting in a 2-dimensional representation. The wavelet analysis function $\psi(t)$ has often referred to as the mother wavelet.

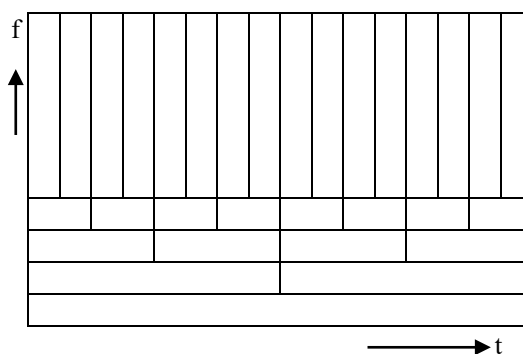


Figure 1 Multiresolution time-frequency plane.

Wavelets

Similar to the FT, the wavelet transform’s [2] evaluating function could have chosen with more flexibility, without the need to use sine-forms. A wavelet function $\psi(t)$ is a small wave that needs to be oscillatory to distinguish between different frequencies somehow. The wavelet includes both the shape and the window of the study. **Figure 2** displays a potential example of a wavelet, known as the Morlet wavelet.

Many kinds of wavelet functions would have built for the CWT (Continuous Wavelet Transform), all of which have particular properties [3,4].

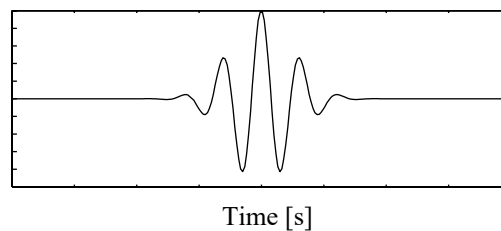


Figure 2 Morlet wavelet.

An analyzing function $\psi(t)$ is classified as a wavelet if the following mathematical criteria are satisfied:

- 1) A wavelet must have finite energy.

$$E = \int_{-\infty}^{\infty} |\psi(f)|^2 dt < \infty. \quad (1)$$

The energy E equals the integrated squared magnitude of the analyzing function $\psi(t)$ and must be less than infinity.

- 2) If $\psi(f)$ is the FT of the wavelet $\psi(t)$, the following condition must hold.

$$C_{\psi} = \int_0^{\infty} \frac{|\psi(f)|^2}{f} dt < \infty. \quad (2)$$

This condition implies that the wavelet has no 0-frequency component ($\psi(0) = 0$), i.e., the mean of the wavelet $\psi(t)$ must equal 0. This condition is known as the admissibility constant. The value of C_{ψ} depends on the chosen wavelet.

- 3) For complex wavelets, the FT $\psi(f)$ must be both real and vanish for negative frequencies.

Continuous wavelet transform

The continuous wavelet transform has defined as:

$$X_{WT}(\tau, s) = \frac{1}{\sqrt{|s|}} \int_{-\infty}^{\infty} x(t) \psi^* \left(\frac{t-\tau}{s} \right) dt. \quad (3)$$

The $X_{WT}(\tau, s)$ transformed signal is a function of the parameter τ of translation and the parameter s of the scale. The * and mother wavelet ψ shows complex conjugate as found in a complex wavelet. As standardized by dividing the wavelet coefficients by $1/\sqrt{|s|}$, the signal energy ensures that every wavelet scale has the same energy.

The mother wavelet would have compressed by increasing the scale parameter s along with dilated. The difference in scale s affects not only the central wavelet frequency f_c but also the window length. Moreover, the scale s is used instead of the frequency to explain the wavelet analysis results. The translation parameter τ determines the wavelet's position in time, which may have changed τ over the signal by shifting the wavelet. For constant scale s and separate translation τ , the time-scale plane's rows have filled in, changing the scale s and holding the language τ occupies the time-scale plane columns continuously. Wavelet coefficients have called the $X_{WT}(\tau, s)$ elements; each wavelet coefficient has correlated with a scale (frequency) and time-domain value. As with the FT and the STFT, the Wavelet Transform also carries an inverse transform. Inverse Continuous Wavelet Transform (ICWT) is defined by:

$$x(t) = \frac{1}{c_{\psi}^2} \int_{-\infty}^{\infty} \int_{-\infty}^{\infty} X_{WT}(\tau, s) \frac{1}{s^2} \psi \left(\frac{t-\tau}{s} \right) \quad (4)$$

Note that the admissibility constant C_ψ must satisfy the 2nd wavelet condition. Within each scale, a wavelet function has its central frequency f_c , and the s value is inversely proportional to that frequency. A large scale corresponds to a low frequency, which gives global signal information. Small sizes equate to high frequencies and provide precise details on the signal. The Heisenberg inequality also holds for the Wavelet Transform, and the bandwidth-time function $\Delta t \Delta f$ is constant and lower bounded. Decreasing s the scale, i.e., a shorter window can increase time resolution as Δt leads to a decreasing resolution of frequencies as Δf . It means that the frequency resolution Δf is equal to the frequency f , i.e., the wavelet analysis's relative frequency resolution is constant. The Morlet wavelet shown in **Figure 2** as derived from a G frame, where f_c is the middle frequency, and f_b is the parameter of bandwidth.

$$\psi(t) = g(t)e^{-j2\pi f_c t}, \quad g(t) = \sqrt{\pi f_b} e^{-t^2/f_b} \tag{5}$$

The center frequency f_c and the bandwidth parameter f_b of the wavelet are the tuning parameters. For the Morlet wavelet, scale and frequency have coupled as $f = f_c/s$.

Discrete wavelet transform

The DWT technique is the age-old signal processing method; it is a mathematical representation or expression having the data [5,6]. Therefore, discrete wavelet transforms as derived from FT, STFT (Short-Time Fourier Transform), FFT (Fast Fourier Transform), DFT (Discrete Fourier Transform), CWT (Continuous Wavelet Transform). The wavelets benefit from the FT since the image can have represented in both frequency attributes of characteristics and spatial domain. Still, FT can be characterized only in frequency attributes of an image.

Wavelets include the properties of orthogonality, translatability, scalability, multiresolution and compatibility. Wavelets offer an improved resolution of a picture for preprocessing as well as a post-processing method. Wavelets afford enough data mutually for analysis and synthesis, decreasing the calculation time satisfactorily, simple to execute and examining the signal at different frequency groups with various declarations. They decompose the indication or signal as a coarse estimation and aspect information, decorate the picture pixels, give high-quality power compaction and be attractive to be orthogonal. Offer adequate data both for analysis as well as synthesis, decrease the calculation time satisfactorily, simple to implement, examine the signal at different frequency groups with different resolutions, decompose the indication or signal as a coarse estimation in addition to aspect information.

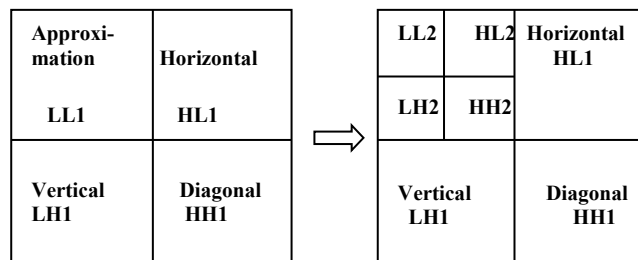


Figure 2 DWT indicating: (a) Decomposition level 1 and (b) Decomposition level 2.

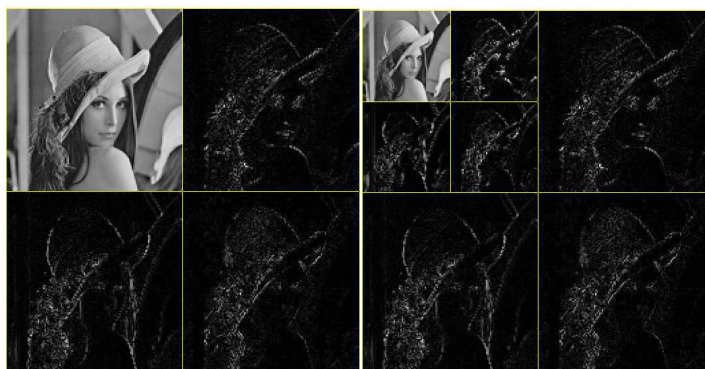


Figure 3 Decomposition levels 1 and 2 Lena standard image.



Figure 4 Reconstruction image of Lena.

Generally, we have split the original image into bands of 4 represented each by LL (Low-Low), HL (High-Low), LH (Low-High) and HH (High-High), which as obtained after single-level decomposition that is said to be single-level decomposition as indicated in **Figure 2(a)**. Further decompositions can have obtained by performing upon the LL sub-band on the succession of the level 1 decomposition. Finally, the resultant single level decomposition image is split into other bands, as indicated in **Figure 2(b)**, respectively. **Figures 3** and **4** gives the representation of decomposition levels approximations and reconstruction or synthesized image[7-9]. after decomposition.

Denoising technique

As **Figure 5** shows, the degradation mechanism since modeled as a degradation function that performs on the input image $f(x, y)$ following an additive noise concept to generate a $g(x, y)$ degraded image. Given $g(x, y)$ some information sequence concerning the degradation function H and some information about the additive noise term $\eta(x, y)$ [10], the restoration objective is to preserve an approximation $\hat{f}(x, y)$ [11-13]of an original image We want the estimate to be as close as possible to the original image, and in general, the more we know about H and η , the closer $\hat{f}(x, y)$ can be to $f(x, y)$. If H is a linear, invariant position operation, the degraded image is represented in the spatial domain by:

$$g(x, y) = h(x, y) * f(x, y) + \eta(x, y). \tag{6}$$

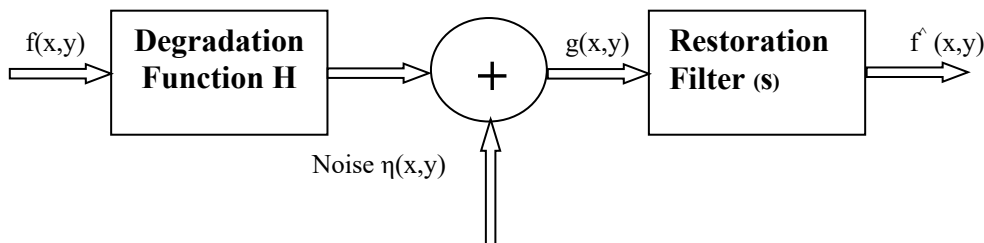


Figure 5 De-noising technique.

Where $h(x, y)$ is the spatial demonstration of the degradation function and, the symbol '*' indicates spatial convolution. Convolution in the spatial domain is similar to multiplication in the frequency domain, such that we can write the model in Eq. (7) in an analogous representation of the frequency domain.

$$G(u, v) = H(u, v)F(u, v) + N(u, v) \tag{7}$$

Noise models, all through image analysis (digitization) and transmission, are the primary source of noise in digital images. During image acquisition, image sensors' output has influenced by several factors such as ambient conditions and the sensing components' efficiency. For instance, light levels and sensor temperature influence the amount of noise in the resulting image when capturing photographs using a CCD (Charged-Couple Device) camera. Images have distorted during transmission primarily due to channel interference used for transmission.

A substantial portion of digital image processing has dedicated to image restoration. It contains investigation in routine goal-oriented and algorithm development image processing. In the image, restoring reduces degradations or removal that as acquired while the image has obtained. Degradation appears from blurring with noise due to electronic elements and photometric sources. Blurring is an appearance of bandwidth decrease of the image caused by the defective image formation method, such as the relative motion between the original scene and the camera or an optical technique to say out of focus. When aerial photography has created for remote sensing, blurs have introduced atmospheric turbulence, irregularity in the optical scheme, and relative motion between ground and camera.

Additionally, to these blurred effects, from noises, the image recorded is corrupted too. The noise is produced in the transmission standard due to a noisy guide and having errors during the whole measuring process and the quantization of data used for digital storage. Every constituent in the imaging chain, such as lenses, film, digitizer and so on, contributes to degradation.

Image denoising is frequently utilized in photography or else publishing anywhere an image has somehow degraded, although its requirements to be improved preceding to it can have printed. For this type of application, we necessitate knowing incredible about the degradation process to develop a model for it. When we include a model used for the degradation process, the inverse process knows how to restore it to the original image form. This image restoration type is repeatedly used in space exploration to remove artifacts generated with mechanical jitter in a spacecraft or else to compensate for distortion of a telescope in the optical system. Image denoising finds application in fields, for example, astronomy wherever the resolution restrictions are severe, in medical imaging wherever the physical requirements designed for high-quality imaging have needed to have used for analyzing images of unique events, and in forensic science where potentially helpful photographic evidence is now and then of terrible quality. The capacity to simulate the behavior with the effects of noise is vital to image restoration. Noise, as added to the original image, is G, S and SP noise.

Gaussian (G) noise

The Probability Density Function (PDF) of a G random variable, z , is given by:

$$p(z) = \frac{1}{2\pi\sigma} e^{-(z - \mu)^2 / 2\sigma^2}. \quad (8)$$

Where z represents the degree of gray level, μ is the mean of an average value of z , and its standard deviation is σ . The standard deviation squared, σ^2 is considered the z variation. G (also known as normal) noise models have frequently are used in practice because of their computational interpretability in both the spatial and frequency domains. This tractability is so simple that it sometimes results in the use of G models in circumstances where they are, at best, partially applicable.

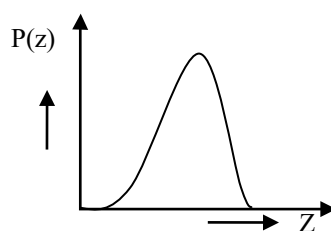


Figure 6 PDF of G noise.

AWGN (Additive White Gaussian Noise) is a simple noise model that uses information theory to reproduce the result from several random processes naturally. The modifiers represent various characteristics:

- 1) Additive as it has applied to any noise which might be intrinsic to the information system.
- 2) White refers to the concept that perhaps the information system provides consistent control across the frequency spectrum. It is an analogy with the white color with constant emissions throughout all frequencies within the visible spectrum.
- 3) G, since it has a time domain of a normal distribution by an average 0 time domain value.

Noise involvement influences the accuracy of the images. The image denoising method attempts to reconstruct and enhance a noiseless image. Denoising an AWGN image is challenging; constraints such as noise variance and mean offer AWGN noise properties.

Salt and Pepper (SP) noise

It has also called Impulse (salt-and-pepper) noise; the PDF of impulse noise is given by:

$$p(z) = \begin{cases} P_a & \text{for } z = a \\ P_b & \text{for } z = b \\ 0 & \text{otherwise} \end{cases} \tag{9}$$

If $b > a$ a gray-level b can appear in the picture as a light dot. On the other hand, level a can look like a dark dot. If either P_a or P_b is 0, the impulse noise is called unipolar, $P(z)$ is PDF, and z is gray. If neither probability is 0, and in particular if they are approximately equal, pulse noise values that resemble randomly scattered SP granules over the picture. Bipolar pulse noise is, therefore, also referred to as SP noise. The terms spike and shot noise as well refer to such noise. The noise impulses have been positive or negative. The scale is usually part of the image digitalization process since impulse corruption is generally high compared to the strength of the image signal, impulse noise as generally digitized as extreme values (pure white or black) in an image. Therefore, the presumption is generally that a and b are “saturated” values in the sense that they are equal to the minimum and maximum allowable values in the digital image. Consequently, negative impulses appear in an image as black (pepper) points. For the same cause, positive impulses illustrate white (salt) noise. This means, to a 8-bit image is referred as (black) $a = 0$ and (white) $b = 255$.

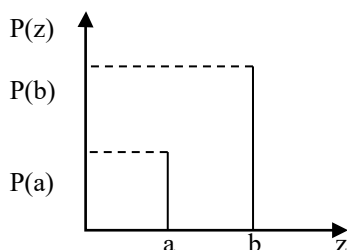


Figure 7 PDF of impulse noise.

Speckle (S) noise

S noise is usually the grainy SP pattern there in radar imagery and S noise can also have interpreted as a granular noise that naturally occurs in as well as degrades the quality of the medical ultrasound, active radar, optical coherence tomography images and synthetic aperture radar. This noise is multiplicative, and S noise in an image can be identical to G noise. The functional probability density resembles the gamma distribution.

$$P(z) = \frac{z^{\alpha-1}}{(\alpha-1)!a^\alpha} e^{-\frac{z}{a}} \tag{10}$$

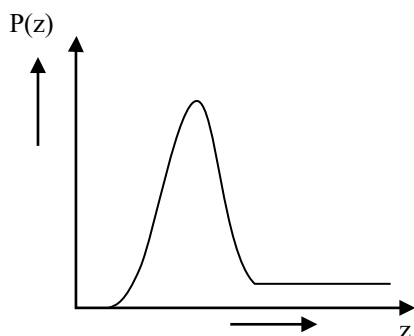


Figure 8 PDF of S noise.

Spatial filtering of image restoration during additive noise

When the only degradation present in an image is noise, Eqs. (6) and (7) become:

$$g(x, y) = f(x, y) + \eta(x, y) \quad (11)$$

$$G(u, v) = F(u, v) + N(u, v) \quad (12)$$

The noise conditions are unknown, and then it is not a practical solution to subtract them from $g(x, y)$ or $G(u, v)$. In the presence of periodic noise, $N(u, v)$, mostly from the spectrum of $G(u, v)$, can typically have calculated. In this case, $N(u, v)$ can have removed from $G(u, v)$ to estimate an original image. For situations whereby the additive noise appears, spatial filters are the method of choice.

Linear filters

In situations where merely additive noise is there, it is the technique of choice. A mean filter[14] is a perfect vector in the form of a mean square error for G noise; therefore, it blurs sharp edges and eliminates lines and other fine image details. It incorporates with Mean and Wiener Filters.

Wiener filter

It is a filter that theoretically approaches the filtering out of signal noise. This filter has used to obtain the desired frequency response. The Wiener filter comes as of a different angle to filter [15,16]. For filtering operations, the spectral characteristics of an original signal and the noise necessity to understand, and the linear time-invariant methods filter[17-19], whose output is as similar as possible to the original signals, can be obtained.

Non-linear filters

In situations where function-based and multiplicative noise[20-23] is present, it is the technique of option. By the non-linear filters, the noise would have eliminated without single detection. In this case, the neighborhood pixel median can decide the output pixel value. Spatial filters use low-pass filtering on pixel classes, meaning that the noise occupies the higher frequency spectrum area. Typically, spatial filters remove noise to a fair degree, but at the expense of blurring images, rendering the edges of images opaque in turn.

Median filter

The Median filter has defined as non-linear, and the median filter is accomplished first by finding the Median value in the window and then by substituting the median value of each entry in the window. If the odd numeral of entries, the median is easy to describe: It is a middle value while in the window, all the entries have numerically sorted. However, there is an additional than one likely median number of entries for an even. It is an efficient filter - the Median filters would have used for smooth image and time-series analysis. The advantage of Median filtering is that it is substantially less responsive than the mean to extreme values (known as outliers). It can eliminate these outliers without decreasing the image sharpness.

Thresholding

Thresholding[24-27] can have defined as the most straightforward technique used for image segmentation. Thresholding is employed to produce binary pictures from grayscale pictures. Global thresholding would have carried out to convert the entropy picture into a binary picture. For the shrinkage and cruder rules, Soft and Hard thresholding [28-30] are the 2 best examples. The hard threshold from any coefficient, which is less than otherwise equivalent to the threshold, is 0. Then Soft thresholding places any threshold as deducted from any coefficient, which is higher than the threshold; also, this shifts the time sequence in the direction of 0.

Measuring parameters

Peak Signal to Noise Ratio (PSNR)

PSNR should be as high as possible since the low PSNR value means that the image quality is poor.

$$\text{PSNR} = 10 \log_{10} \frac{255^2}{\text{MSE}} \quad (13)$$

Mean Squared Error (MSE)

The high value of MSE indicates that an image is of low quality.

$$MSE = \frac{\sum_{m,n} [I_1(m,n) - I_2(m,n)]^2}{M*N} \tag{14}$$

**Image denoising methodology
Without a mixture of the noise model**



Figure 9 Block diagram of image denoising.

Figure 9 shows preprocessing, and noise added, denoising, Median filter, Wiener filter and PSNR & MSE. In preprocessing, the input image resized 512×512 of grayscale in jpeg format; to this image, noise density 10 % is added such as G, S and SP for assessing. Then it is denoised using different wavelets by DWT keeping decomposition level-2; at HT (Hard Thresholding) and ST (Soft Thresholding) [31-33] of having threshold value is equal to 100, further, it as used to reduce noise by Median and Wiener filters, and therefore checked image quality by PSNR and MSE.

With a mixture of the noise model

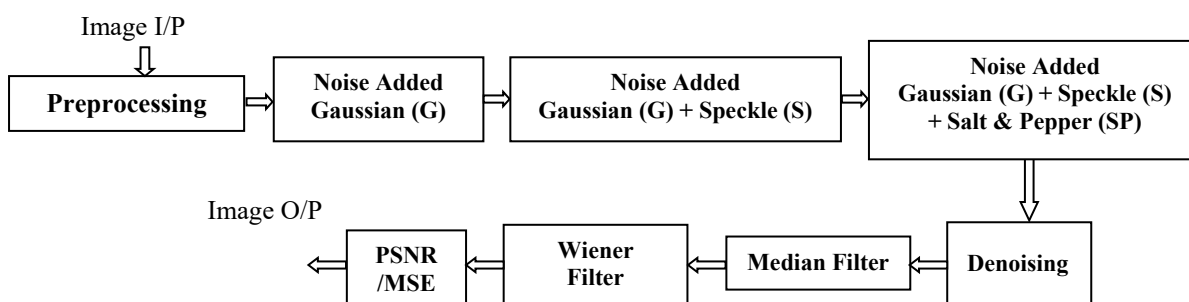


Figure 10 Mixture of noise image denoising.

There are different methods to help out restore an image from the noisy distortions. Selecting a suitable technique plays the most crucial role in getting the nearer original desired image. The denoising methods tend to be problem-specific. For example, a technique used to denoise images[34,35] could not be appropriate for denoising all the images. A study was made on the denoising algorithm and implemented to Lena image data information in this examination work. Some known noise would have added to an image taken to analyze the denoising algorithm’s efficiency. Subsequently, this would have provided the same input to the denoising algorithm, which produces an image the same as the original one.

Gaussian = (G), Gaussian + Speckle = (G + S), Gaussian + Speckle + Salt and Pepper = G + S + SP, additive mixture of noise distribution of probability noise density 0.1, 1 and 10 % have used in this exploratory.

The model proposes noise signal removal from the images to obtain better performance when the noise is asymmetrical. It is challenging to perform methodology for an additive mixture of noise distribution during sensitivities towards the external and internal components. It is a multidimensional filtering technique to enhance an image or depends upon the significance of features in an image of noise removal. A model affected by the system may be symmetrical or asymmetrical noise distribution in transmission to retrieve as the original image.

As shown in **Figure 10**, processing as similar to **Figure 9** only mixture of noise has added to the image that is G + S + SP (Gaussian + Speckle + Salt and Pepper), the image is corrupted of noise density 0.1, 1 and 10 %, and it is denoised by different wavelets with spatial filters.

Algorithm for denoising with noise

- Step 1: Start
 Step 2: Input image Lena, jpeg format, load the source image data from a file into an array
 Step 3: Preprocessing- resized to 512×512, grayscale
 Step 4: With noise to the source image data, add noise G or S or SP or (G + S + SP)
 Step 5: Choose the wavelet, using Sevenlets Wavelet are Haar or Daubechies or Coiflets or Symlets or Discrete Meyer or Biorthogonal or Reverse Biorthogonal
 Step 6: Compute the wavelet decomposition of signals at level N
 Step 7: Thresholding is applied to the detail coefficients, for each level from 1 to N, at hard and soft thresholding
 Step 8: Compute Wavelet reconstruction, denoised, if YES goto step-11, if NO goto step-9
 Step 9: Median filter to reduce the noise, if YES goto step-11, if NO goto step-10
 Step 10: Wiener filter to reduce the noise and blurring of an image
 Step 11: PSNR/MSE to check the image quality
 Step 12: End

Results and discussion

Lena standard image with G noise

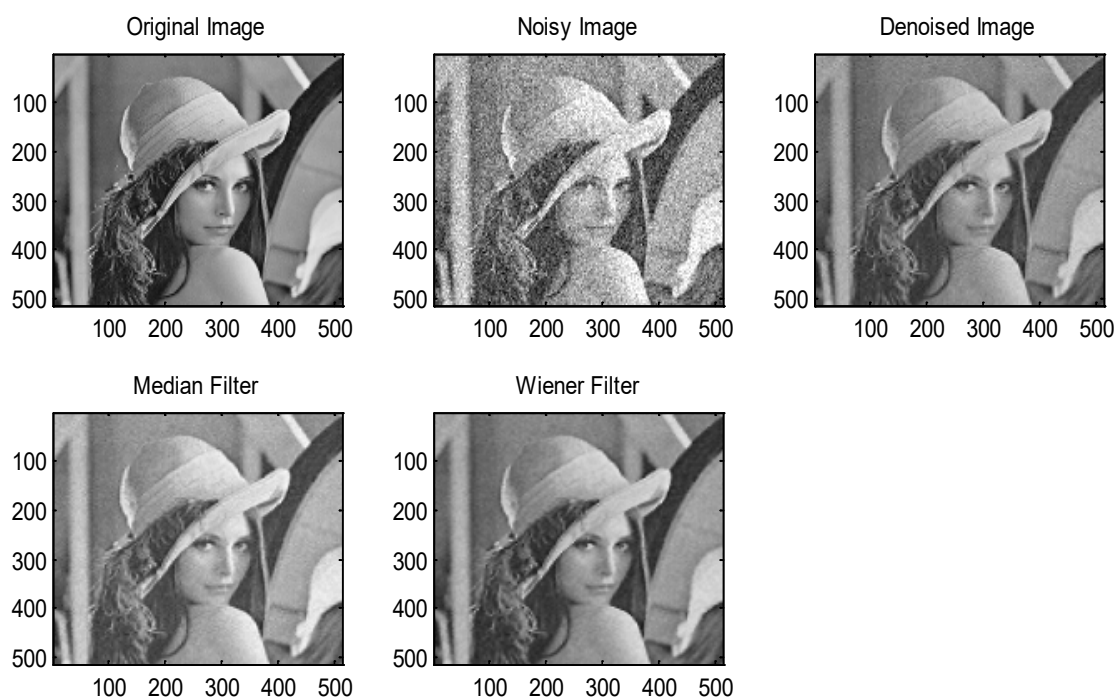


Figure 11 Lena standard image with G noise from left to right: (a) Original image, (b) Noisy image, (c) Denoised image, (d) Wiener filter image and (e) Median filter image.

Table 1 Lena standard image with G noise for HT and ST.

| Threshold | Wavelet | Denoising | | Median | | Wiener | |
|-----------|---------|-----------|--------|--------|--------|--------|--------|
| | | PSNR | MSE | PSNR | MSE | PSNR | MSE |
| HT | haar | 44.53 | 756.82 | 44.79 | 765.16 | 45.03 | 719.78 |
| | db2 | 44.90 | 729.46 | 45.18 | 709.80 | 45.22 | 706.58 |
| | coif2 | 45.03 | 720.32 | 45.20 | 707.75 | 45.28 | 702.47 |
| | sym4 | 45.06 | 717.84 | 45.23 | 706.08 | 45.32 | 699.49 |
| | dmey | 45.12 | 713.98 | 45.23 | 706.06 | 45.35 | 697.66 |
| | bior6.8 | 45.06 | 717.86 | 45.20 | 707.88 | 45.30 | 701.36 |
| | rbio6.8 | 45.08 | 716.55 | 45.26 | 703.93 | 45.36 | 696.60 |
| ST | haar | 44.40 | 766.80 | 44.64 | 748.21 | 44.87 | 731.19 |
| | db2 | 44.88 | 730.98 | 45.11 | 714.59 | 45.16 | 710.72 |
| | coif2 | 44.99 | 723.25 | 45.12 | 713.64 | 45.21 | 707.33 |
| | sym4 | 44.92 | 727.86 | 45.05 | 718.44 | 45.16 | 711.14 |
| | dmey | 45.07 | 716.88 | 45.16 | 710.61 | 45.27 | 702.79 |
| | bior6.8 | 45.02 | 720.68 | 45.13 | 712.98 | 45.23 | 706.25 |
| | rbio6.8 | 44.99 | 723.08 | 45.11 | 714.67 | 45.21 | 707.29 |

The external G noise is added 10 % density to the image, at different wavelets it is processed. The denoised and Median & Wiener filters having good quality image generated as shown in **Figure 11**, from **Table 1** the PSNR and MSE is marginally different for all the wavelets efficiency, performance is better for both soft and hard thresholding; when a threshold value is equal to 100.

Lena standard image with S noise

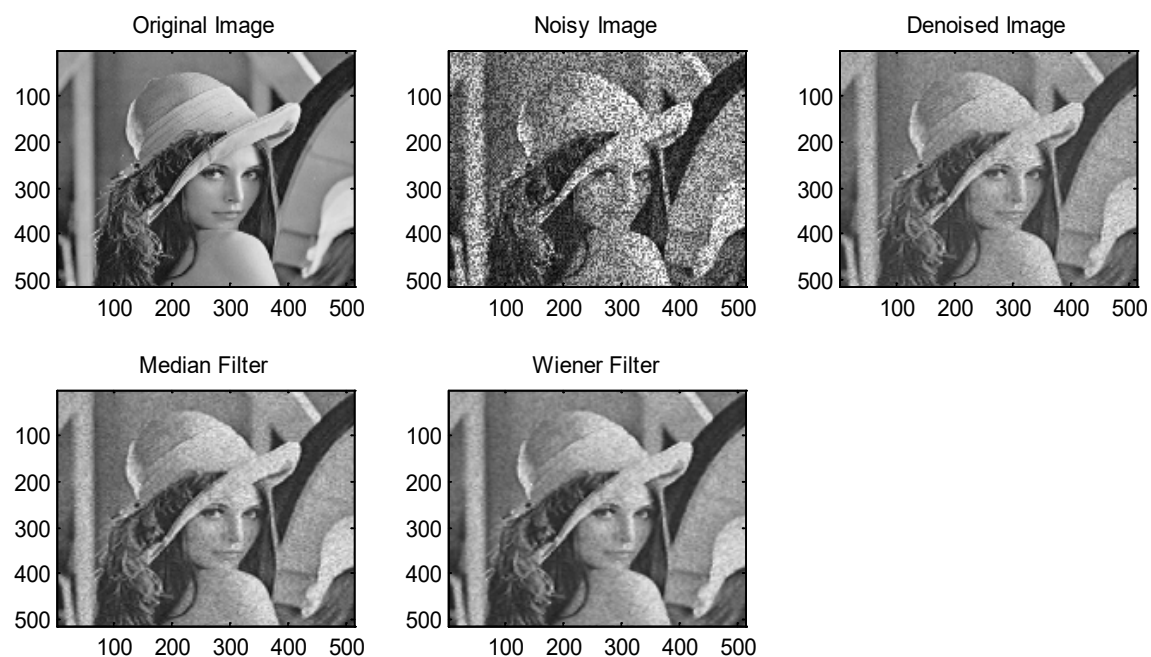


Figure 12 Lena standard image with S noise from left to right: (a) Original image, (b) Noisy image, (c) Denoised image, (d) Wiener filter image and (e) Median filter image.

Table 2 Lena standard image with S noise for HT and ST.

| Threshold | Wavelet | Denoising | | Median | | Wiener | |
|-----------|---------|-----------|--------|--------|--------|--------|--------|
| | | PSNR | MSE | PSNR | MSE | PSNR | MSE |
| HT | haar | 49.49 | 461.26 | 57.07 | 216.02 | 57.44 | 208.27 |
| | db2 | 50.67 | 409.62 | 60.63 | 151.33 | 58.15 | 193.86 |
| | coif2 | 50.54 | 414.96 | 60.11 | 159.36 | 58.09 | 195.09 |
| | sym4 | 50.61 | 412.06 | 60.20 | 157.92 | 58.11 | 194.63 |
| | dmey | 50.26 | 426.97 | 59.64 | 167.11 | 58.19 | 193.04 |
| | bior6.8 | 50.28 | 425.96 | 59.40 | 172.12 | 57.95 | 197.77 |
| | rbio6.8 | 49.94 | 440.71 | 60.14 | 158.92 | 57.93 | 198.21 |
| ST | haar | 57.70 | 202.74 | 59.46 | 170.14 | 61.99 | 132.13 |
| | db2 | 59.52 | 169.14 | 62.24 | 128.81 | 63.48 | 113.84 |
| | coif2 | 60.06 | 160.26 | 62.11 | 130.53 | 63.86 | 109.55 |
| | sym4 | 59.92 | 162.40 | 61.91 | 133.20 | 63.69 | 111.48 |
| | dmey | 60.38 | 155.16 | 62.08 | 130.87 | 64.22 | 105.59 |
| | bior6.8 | 59.93 | 162.32 | 61.72 | 135.75 | 63.79 | 110.32 |
| | rbio6.8 | 59.94 | 162.22 | 61.89 | 133.46 | 63.88 | 109.38 |

As shown in **Figure 12**, to the Lena image a S noise is introduced with a 10 % density noise level, image is denoised and then filtered by Median and Wiener, From **Table 2**, performance varies during HT and ST, can be identified by PSNR and MSE analysis. At soft thresholding, MSE is low comparing with hard thresholding. Image quality is moderate and better to analyze, edges can identify with clarity.

Lena standard image with SP noise

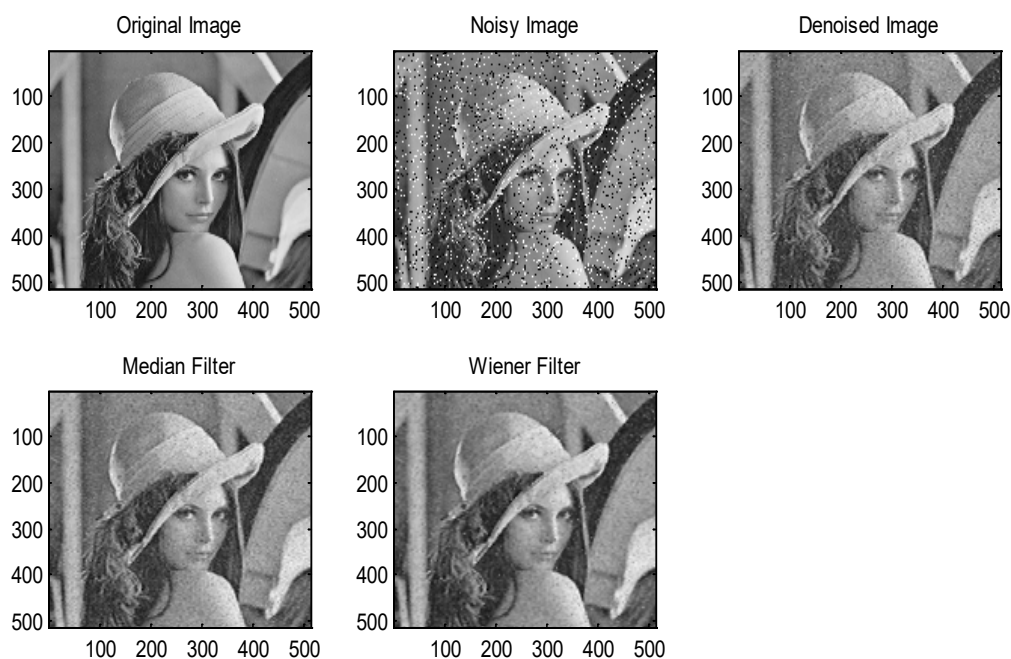


Figure 13 Lena standard image with SP noise from left to right: (a) Original image, (b) Noisy image, (c) Denoised image, (d) Wiener filter image and (e) Median filter image.

Table 3 Lena standard image with SP noise for HT and ST.

| Threshold | Wavelet | Denoising | | Median | | Wiener | |
|-----------|---------|-----------|--------|--------|--------|--------|--------|
| | | PSNR | MSE | PSNR | MSE | PSNR | MSE |
| HT | haar | 43.59 | 831.36 | 59.34 | 172.21 | 51.81 | 365.73 |
| | db2 | 42.74 | 905.59 | 60.95 | 146.61 | 53.40 | 311.73 |
| | coif2 | 44.11 | 789.69 | 60.59 | 151.95 | 54.36 | 283.40 |
| | sym4 | 44.09 | 791.30 | 60.81 | 148.64 | 54.12 | 290.11 |
| | dmey | 45.95 | 657.08 | 59.97 | 161.60 | 55.25 | 259.31 |
| | bior6.8 | 44.39 | 767.89 | 59.90 | 162.77 | 54.10 | 290.86 |
| | rbio6.8 | 44.31 | 773.83 | 60.46 | 153.93 | 54.37 | 282.95 |
| ST | haar | 55.17 | 261.20 | 58.42 | 188.70 | 59.37 | 171.66 |
| | db2 | 55.81 | 245.05 | 60.78 | 149.14 | 60.43 | 154.43 |
| | coif2 | 56.48 | 229.13 | 60.62 | 150.77 | 60.67 | 150.48 |
| | sym4 | 56.72 | 223.65 | 60.61 | 151.69 | 60.79 | 148.98 |
| | dmey | 57.88 | 199.29 | 60.76 | 149.33 | 61.56 | 137.92 |
| | bior6.8 | 57.03 | 217.03 | 60.68 | 150.66 | 61.03 | 145.48 |
| | rbio6.8 | 56.76 | 222.88 | 60.54 | 152.75 | 60.88 | 147.66 |

As shown in **Figure 13**, the original image is corrupted by adding SP noise of 10 % density level. From **Table 3** the performance at ST of MSE is reduced comparing to HT and PSNR is better at ST. Hence image quality is improved for both Hard and Soft thresholding for all the wavelets that have observed images when a threshold value is equal to 100.

SP noise when threshold value is 1

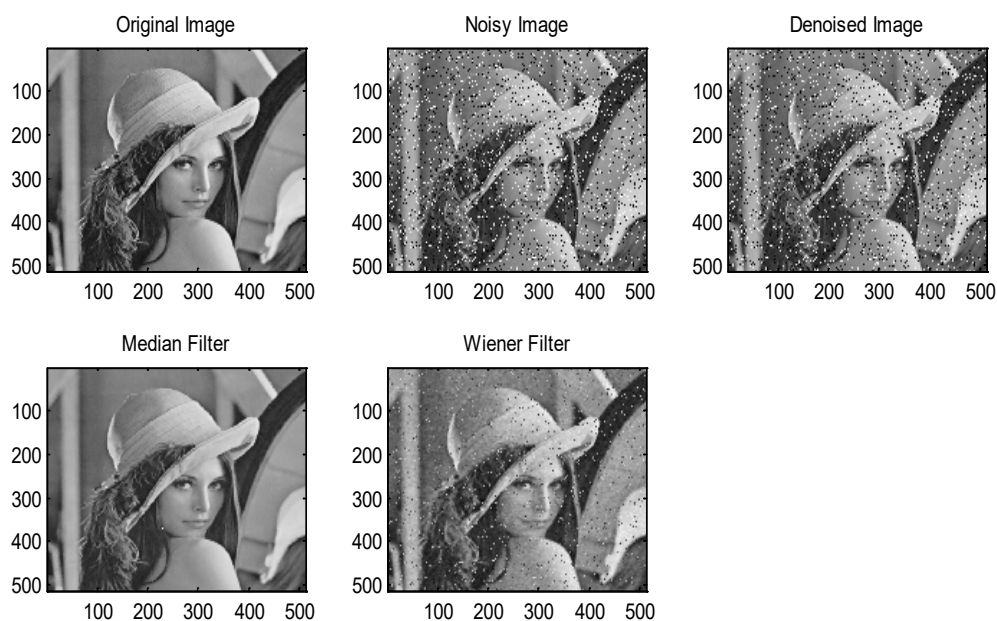


Figure 14 Lena standard image with SP noise from left to right: (a) Original image, (b) Noisy image, (c) Denoised image, (d) Wiener filter image and (e) Median filter image.

Table 4 Lena standard image with SP noise for HT and ST.

| Threshold | Wavelet | Denoising | | Median | | Wiener | |
|-----------|---------|-----------|--------|--------|-------|--------|--------|
| | | PSNR | MSE | PSNR | MSE | PSNR | MSE |
| HT | haar | 35.62 | 1846.1 | 83.25 | 15.76 | 52.43 | 343.48 |
| | db2 | 35.53 | 1859.1 | 82.30 | 17.33 | 52.05 | 356.81 |
| | coif2 | 35.48 | 1872.3 | 80.48 | 19.86 | 52.07 | 356.32 |
| | sym4 | 35.55 | 1858.7 | 82.00 | 17.84 | 52.16 | 353.06 |
| | dmey | 35.66 | 1837.8 | 81.91 | 18.02 | 52.21 | 351.24 |
| | bior6.8 | 35.48 | 1870.7 | 81.42 | 18.92 | 52.04 | 357.37 |
| | rbio6.8 | 35.66 | 1837.5 | 82.34 | 17.26 | 52.30 | 347.96 |
| ST | haar | 35.82 | 1808.5 | 81.84 | 18.14 | 52.36 | 346.00 |
| | db2 | 35.87 | 1799.1 | 81.80 | 18.23 | 52.39 | 345.16 |
| | coif2 | 35.92 | 1790.6 | 82.82 | 16.45 | 52.39 | 345.11 |
| | sym4 | 35.86 | 1802.3 | 82.05 | 17.77 | 52.43 | 343.67 |
| | dmey | 35.74 | 1822.9 | 81.65 | 18.50 | 52.02 | 358.04 |
| | bior6.8 | 35.84 | 1805.8 | 80.78 | 20.17 | 52.26 | 349.50 |
| | rbio6.8 | 35.89 | 1796.2 | 82.09 | 17.70 | 52.29 | 348.60 |

When the threshold value is equal to 1, during SP noise is added to the image as shown in **Figure 14**, at median filter performance is excellent for both hard and soft thresholding then comparing to the denoising and Wiener filter from **Table 4**. At ST and HT values are almost similar differences for 7 wavelets filters. As minimizes the threshold value for SP noise at Median filter processing, obtained better clarity image than Weiner and denoising process.

Denoising with mixed noise

Lena image with mixed noise density is 0.1 %

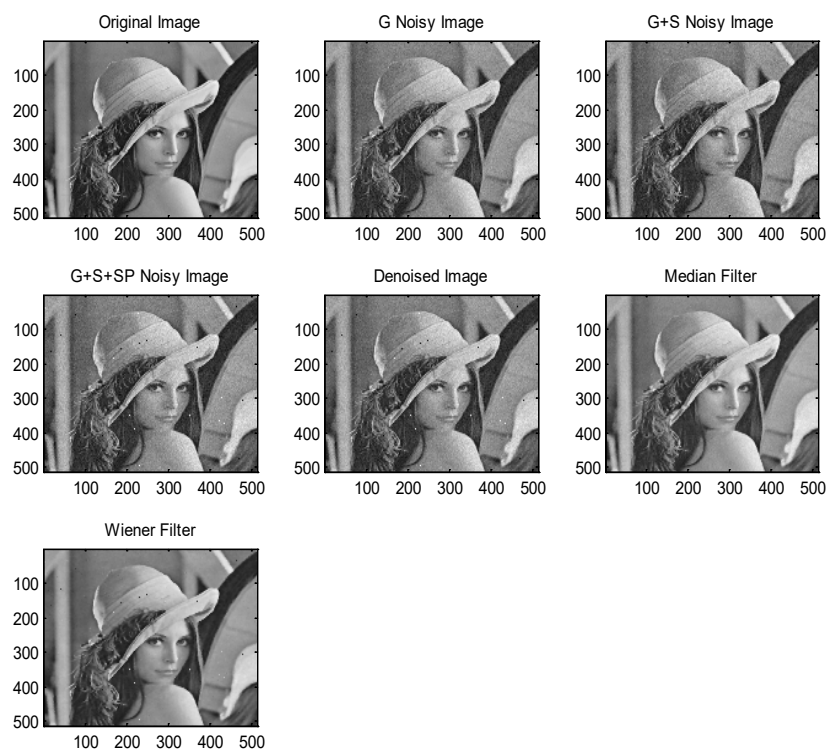


Figure 15 Lena with mixed noise 0.1 % (G + S + SP): (a) Original image, (b) G noise image, (c) (G + S) Noise image, (d) (G + S + SP) Noise image, (e) Denoised filter, (f) Median image and (g) Wiener filter.

Table 5 Lena with mixed noise (G + S + SP) density 0.1 %.

| Threshold | Wavelet | Denoising | | Median | | Wiener | |
|-----------|---------|-----------|-------|--------|-------|--------|-------|
| | | PSNR | MSE | PSNR | MSE | PSNR | MSE |
| HT | haar | 66.04 | 88.10 | 79.20 | 23.63 | 75.20 | 34.69 |
| | db2 | 65.96 | 88.79 | 79.34 | 23.31 | 75.21 | 35.21 |
| | coif2 | 66.13 | 87.33 | 79.33 | 23.32 | 75.37 | 34.65 |
| | sym4 | 65.79 | 90.31 | 79.36 | 23.26 | 74.78 | 36.79 |
| | dmey | 65.84 | 89.89 | 79.34 | 23.31 | 74.95 | 36.13 |
| | bior6.8 | 65.89 | 89.42 | 79.31 | 23.38 | 74.93 | 36.13 |
| | rbio6.8 | 66.27 | 86.12 | 79.67 | 23.47 | 75.60 | 33.86 |
| ST | haar | 66.02 | 88.20 | 79.17 | 23.70 | 75.27 | 35.01 |
| | db2 | 65.92 | 89.18 | 79.87 | 23.43 | 75.03 | 35.87 |
| | coif2 | 65.91 | 89.27 | 79.36 | 23.26 | 75.12 | 35.53 |
| | sym4 | 66.10 | 87.55 | 79.36 | 23.25 | 75.25 | 35.01 |
| | dmey | 66.06 | 87.93 | 79.31 | 23.38 | 75.32 | 34.82 |
| | bior6.8 | 65.88 | 89.55 | 79.29 | 23.41 | 75.01 | 35.93 |
| | rbio6.8 | 65.98 | 88.61 | 79.31 | 23.37 | 75.23 | 35.16 |

The mixer of noise density 0.1 % is introduced into the image as shown in **Figure 15**, the G, S, and SP are added to Lena's original image. Noise level is reduced in the images. From **Table 5** the MSE is minimized and PSNR is fine at ST and HT when a threshold value is 100. At the Median filter, the PSNR is better and MSE is reduced comparing to the denoising and Wiener filter. As a mixer of noise is added when noise density is low image clarity is excellent.

Lena image with mixed noise density is 1 %

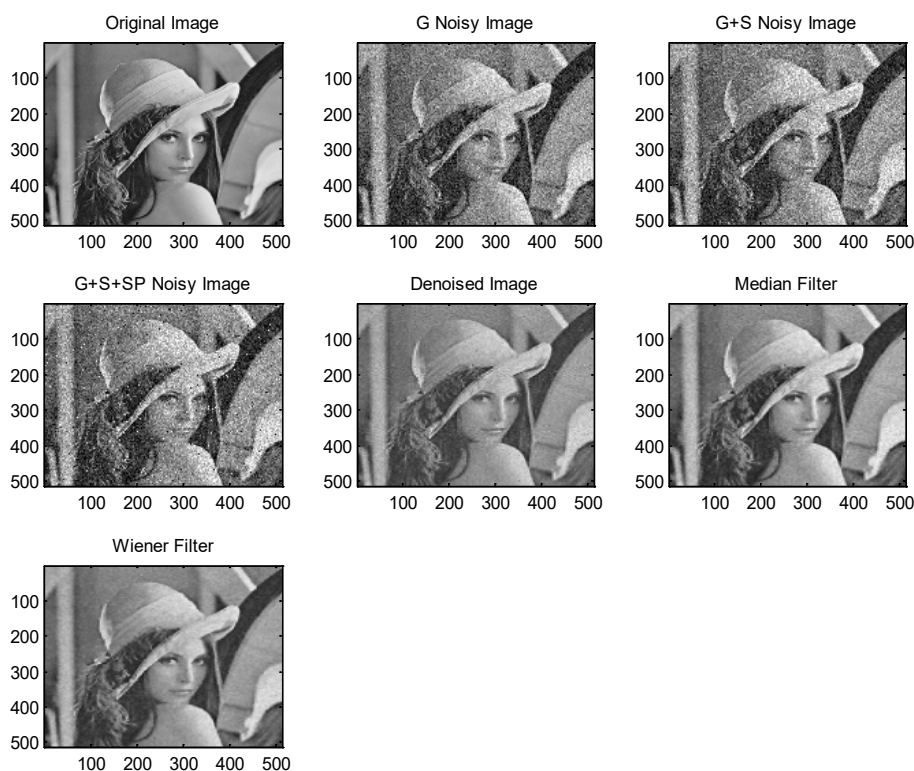


Figure 16 Lena with mixed noise 1 % (G + S + SP): (a) Original image, (b) G noise image, (c) (G + S) noise image, (d) (G + S + SP) noise image, (e) Denoised image, (f) Median filter and (g) Wiener filter.

Table 6 Lena with mixed noise (G + S + SP) density 1 %.

| Threshold | Wavelet | Denoising | | Median | | Wiener | |
|-----------|---------|-----------|--------|--------|--------|--------|--------|
| | | PSNR | MSE | PSNR | MSE | PSNR | MSE |
| HT | haar | 60.57 | 152.30 | 62.22 | 129.10 | 64.18 | 106.11 |
| | db2 | 62.84 | 121.33 | 65.25 | 95.31 | 66.00 | 88.45 |
| | coif2 | 63.72 | 111.12 | 65.39 | 94.01 | 66.60 | 83.32 |
| | sym4 | 63.85 | 109.69 | 65.41 | 93.82 | 66.60 | 83.30 |
| | dmey | 64.55 | 102.27 | 65.60 | 92.08 | 67.23 | 78.23 |
| | bior6.8 | 64.23 | 105.53 | 65.54 | 92.67 | 66.96 | 80.34 |
| | rbio6.8 | 63.87 | 109.50 | 65.33 | 94.61 | 66.86 | 81.18 |
| ST | haar | 60.55 | 152.54 | 62.23 | 128.90 | 64.20 | 105.94 |
| | db2 | 62.96 | 119.88 | 65.42 | 93.75 | 66.20 | 86.71 |
| | coif2 | 63.79 | 110.37 | 65.44 | 93.51 | 66.64 | 82.98 |
| | sym4 | 63.80 | 110.26 | 65.37 | 94.24 | 66.70 | 82.51 |
| | dmey | 64.54 | 102.36 | 65.61 | 92.01 | 67.26 | 78.01 |
| | bior6.8 | 64.06 | 107.43 | 65.38 | 94.12 | 66.84 | 81.29 |
| | rbio6.8 | 63.89 | 109.24 | 65.37 | 94.25 | 66.86 | 81.18 |

As the mixer of noise is increased at a density level of 1 %, MSE increasing and PSNR marginally decreases, as shown in **Figure 16** image clarity is satisfactory. From **Table 6** at Wiener filter, PSNR is better and MSE is low comparing with denoising and Median filter. The performance is satisfactory at a 1 % density noise mixer level.

Lena image with mixed noise density is 10 %

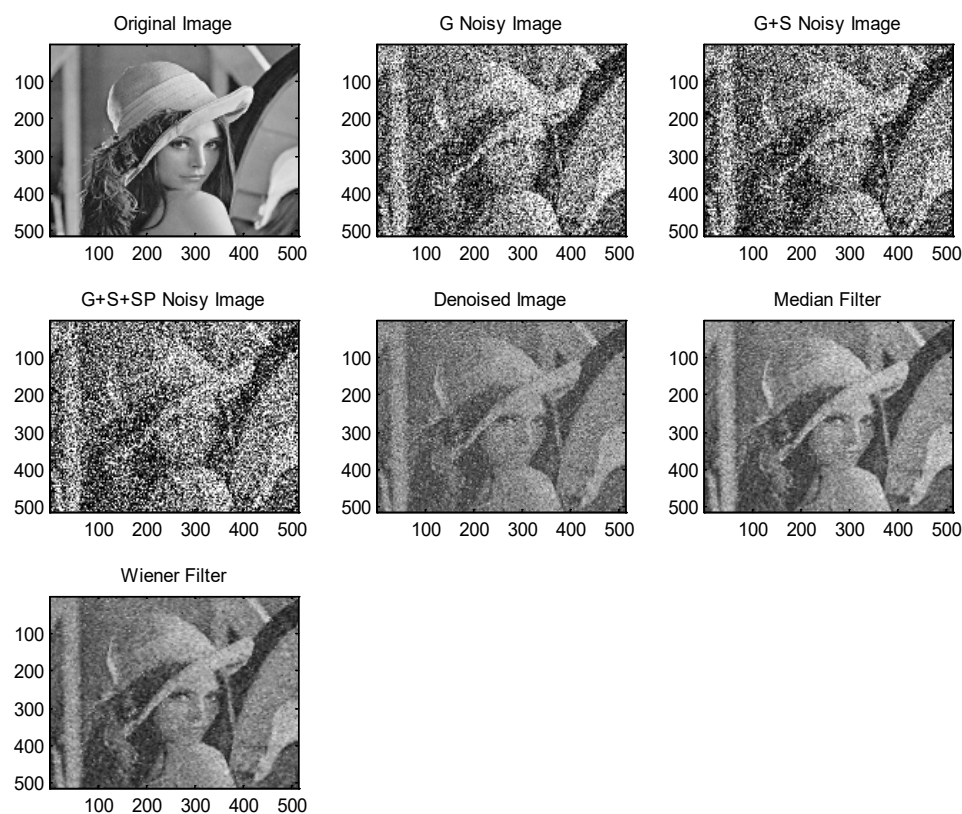


Figure 17 Lena with mixed noise 10 % (G + S + SP): (a) Original image, (b) G Noise image, (c) (G + S) Noise image, (d) (G + S + SP) Noise image, (e) Denoised image, (f) Median filter and (g) Wiener filter.

Table 7 Lena with mixed noise (G + S + SP) density 10 %.

| Threshold | Wavelet | Denoising | | Median | | Wiener | |
|-----------|---------|-----------|---------|--------|--------|--------|--------|
| | | PSNR | MSE | PSNR | MSE | PSNR | MSE |
| HT | haar | 39.71 | 1226.3 | 45.51 | 686.45 | 47.41 | 567.45 |
| | db2 | 39.99 | 1191.2 | 46.42 | 626.77 | 47.47 | 564.39 |
| | coif2 | 40.04 | 1185.7 | 46.15 | 643.59 | 47.50 | 562.65 |
| | sym4 | 40.03 | 1187.5 | 46.10 | 647.27 | 47.47 | 564.24 |
| | dmey | 39.91 | 1202.3 | 45.77 | 669.01 | 47.37 | 570.14 |
| | bior6.8 | 39.94 | 1198.1 | 45.88 | 661.77 | 47.40 | 568.07 |
| | rbio6.8 | 39.74 | 1.222.0 | 46.03 | 651.71 | 47.39 | 568.96 |
| ST | haar | 39.79 | 1216.2 | 45.65 | 676.71 | 47.50 | 562.39 |
| | db2 | 40.10 | 1179.5 | 46.59 | 616.32 | 47.61 | 556.26 |
| | coif2 | 40.05 | 1185.2 | 46.16 | 643.45 | 47.48 | 563.54 |
| | sym4 | 40.04 | 1186.2 | 46.09 | 647.68 | 47.47 | 564.15 |
| | dmey | 39.94 | 1198.3 | 45.82 | 665.78 | 47.39 | 569.07 |
| | bior6.8 | 39.80 | 1215.1 | 45.64 | 677.60 | 47.23 | 577.93 |
| | rbio6.8 | 39.74 | 1215.1 | 46.03 | 651.48 | 47.42 | 567.07 |

For mixer of noise density level is 10 % the performance is not satisfactory, MSE is very high and PSNR is lower for all the wavelets at denoising, Median and Wiener filter as shown in **Figure 17** and **Table 7**. At Wiener filter comparing to denoising and Median filter is modest.

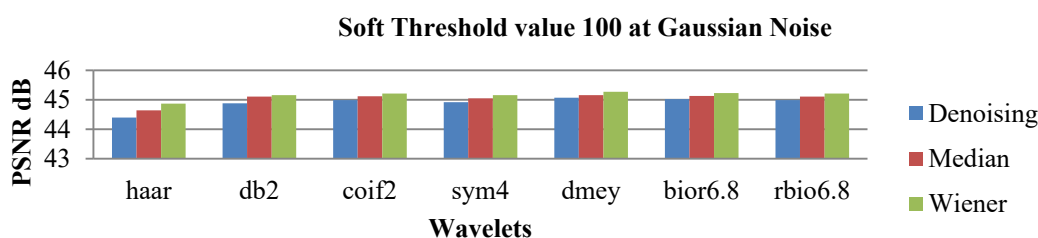


Figure 18 Soft thresholding for value 100 at G noise.

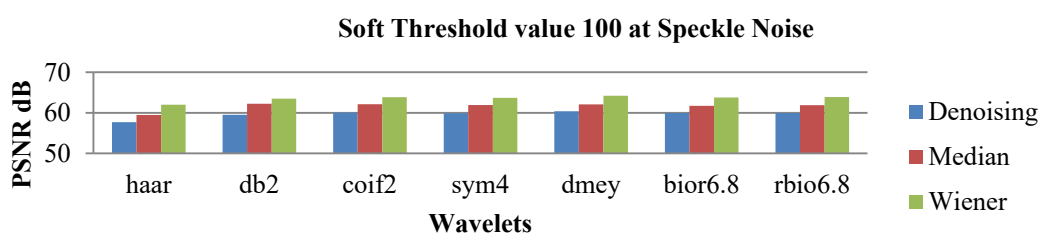


Figure 19 Soft thresholding for value 100 at S noise.

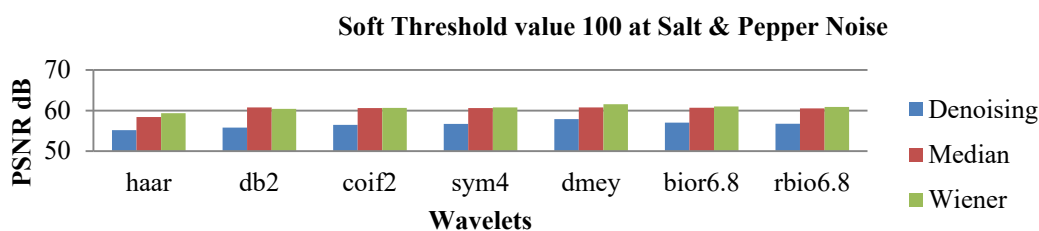


Figure 20 Soft thresholding for value 100 at SP noise.

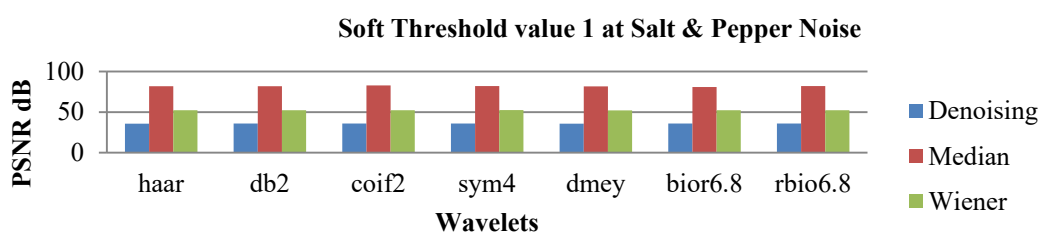


Figure 21 Soft thresholding for value 1 at SP noise.

The noise 10% density as added to the images to Sevenlets wavelet shows image quality, as shown in **Tables 1 - 4** and plots **Figures 18 - 21**. At denoising of images for HT and ST having high MSE and low PSNR, at the Median, and Wiener filters improved PSNR and reduced MSE. Both HT and ST is having better results. For G and S noise, the Wiener filter is excellent than the Median filter. At SP noise, the Median filter performance is superior then the Wiener, satisfactory to other noise. At a higher threshold level, the Median filter performance not better for SP but a lesser threshold is excellent in reducing the noise. The number of decomposition levels should be less otherwise image will be blurred, in this research decomposition level is 2 for all the experiments.

As shown in **Figures 15 - 17** and **Tables 5 - 8**, the inquisition is on a mixed noise level during transmission level or communication systems; due to electronics modules, the image with noise may have corrupted. Hence, the Lena standard image was noise added and examined a novel approach by adding the mixed type of noise: G + S + SP. Percentage of noise density added in the sequence of 0.1, 1 and 10 %, quality of image checked by PSNR and MSE. It would have found that as the percentage of noise density is increasing, the image quality clarity decreases. After an image is denoised by the wavelet technique at decomposition level 2, HT, and ST of the threshold as value 100, the filters used are Median and Wiener filters to reduce the image's noise level. However, the Wiener filters having higher PSNR and lower MSE than the Median. After filters were applied to the denoised image, the quality has improved with clarity for low density mixed noise. As noise density increases, the performance decreases for both Median and Wiener filters.

From comparing values from the tables, the PSNR values would have calculated by subtracting from the original to the output image to definite improvement in the image, and errors present in the image are known accurately. It would have observed that to get higher PSNR if the output subtracted from the noisy image results is different; it is not correct processing or method. Many researchers compared results from the added noisy and output image. It should be output, and the original: The image to be evaluated and retrieved similar to the original image in the medical image processing plays a vital role in diagnosis without any maximum loss of information. The loss of data is a severe concern for the identification of contours or edges of any format. The analysis should not be on a compromise basis; it should be precise quantitative and qualitative analysis. It is a question of the medical image or any standard image; the accuracy is the main target to obtain excellent retrieving as the original. As shown from **Table 7** comparison of previous methods results respective to noise, achieved better performance in this exploration work.

Table 8 Comparison of research results with previous methods from the literature.

| Author | PSNR dB | | |
|---|--------------|--------------|---------------|
| | Gaussian | Speckle | Salt & Pepper |
| Kommineni and Kalluri [6] | 15.54 | 16.30 | 19.17 |
| Setu Garg et al., Median filter [31] | 18.33 | 21.90 | 28.21 |
| Setu Garg et al., Wiener filter [31] | 17.13 | 22.55 | 22.22 |
| Hu <i>et al.</i> [34] | | | 35.90 |
| Aydikia <i>et al.</i> [35] | 20.35 | | 26.43 |
| Research achieved at Median filter on Lena image | 44.53 | 49.49 | 83.25 |
| Research achieved at Wiener filter on Lena image | 45.29 | 55.66 | 52.44 |

Conclusions

In this novelty, 7 wavelets used given behavior with noises by wavelet transform. Spatial filters operate by smoothing over a fixed window, and it produces artifacts around the object and sometimes causes over smoothing, thus causing blurring of the image. Therefore, Wavelet transform is best suited for performance because of its properties like sparsity, multiresolution and multiscale nature. PSNR and MSE values as also calculated for different wavelet families. Recently, image denoising in the wavelet domain attracts much attention in image and signal processing. Optimized based noise removal methods have good results, but the quality of an image needs to be enhanced, restored and improved. Noise removal in Lena jpeg format case using the standard methods to remove complexity without over smoothing and blurring images; significantly, the image quality of clarity should not compromise while increasing parameter measurement. In digital image processing, lossless data information very significant and vital to retrieving accurately. Wavelets have helped the image be multiresolution to obtain exceptional clarity when used Median and Wiener filters. Adding 3 types of noises such as G, S and SP also a mixture of noise (G + S + SP) to image as examined in this inquest, given quantitative and qualitative analysis, the Median filter performs better for SP noise removal at the lower threshold. It is found that for low noise density excellent for a mixture of noise; the Wiener filter produces better performance for a less density mixture of noise and has an adaptive behavioral response. This research provides fine results for higher density noise removal with a novel approach for a mixture of noise.

Future scope

Various issues can have addressed by image processing and computer vision. Based on such criteria, thorough research and development for each application have superior, i.e., advancement in imaging methods, progress, in theory, expansion of computing capacity, therefore presently emerging and need for development and explore in these areas while keeping these criteria in mind. Based on the investigation fields, these technologies are classified; the related possibilities of various opportunities in image processing using wavelets for future enhancement, in the field of satellite communication engineering to eliminate noise at the transmitters and receivers during the uploading and downloading images, in medical diagnosis to obtain exact imagery because of noise will be present due to electronics equipment, in the field of agriculture sector such as seed investigation denoising, this investigation can be extended using different image formats for chromatic and non-chromatic at linear and non-linear filtering methods as per requirement.

References

- [1] L Fan, F Zhang, H Fan and C Zhang. Brief review of image denoising techniques. *Vis. Comput. Ind. Biomed. Art* 2019; **2**, 7.
- [2] G Kaur and R Kaur. Image denoising using wavelet transform and various filters. *Int. J. Res. Comput. Sci.* 2012; **2**, 15-21.
- [3] P Koranga, G Singh, D Verma, S Chaube, A Kumar and S Pant. Image denoising based on wavelet transform using visu thresholding technique. *Int. J. Math. Eng. Manag. Sci.* 2018; **3**, 444-9
- [4] L Singh and R Janghel. *Image denoising techniques: A brief survey*. In: Harmony search and nature inspired optimization algorithms. Springer, Singapore, 2018, p. 731-40.
- [5] PB Alisha and KG Sheela. Image denoising techniques - an overview. *J. Electron. Commun. Eng.* 2016; **11**, 78-84.

- [6] VRR Kommineni and HK Kalluri. Image denoising techniques. *Int. J. Recent Technol. Eng.* 2019; **7**, 417-9.
- [7] J Wang, J Wu, Z Wu, J Jeong and G Jeon. Wiener filter-based wavelet domain denoising. *Displays* 2017; **46**, 37-41.
- [8] SK Agarwal and P Kumar. Denoising of a mixed noise color image through special filter. *Int. J. Signal Process.* 2016; **9**, 159-76.
- [9] Alka Yadav, Naveen Dewangan and Subra Debdas. Wavelet for ECG Denoising using Multiresolution Technique. *In. J. Sci. & Engg. Res.* 2012; **3**, 1-3.
- [10] Y Qian. Removing of salt-and-pepper noise in images based on adaptive Median filtering and improved threshold function. *In: Proceedings of the 2019 Chinese Control and Decision Conference, Nanchang, China.* 2019, p. 1431-6.
- [11] R Dass. Speckle noise reduction of ultrasound images using BFO cascaded with Wiener filter and discrete wavelet transform in homomorphic region. *Procedia Comput. Sci.* 2018; **132**, 1543-51.
- [12] A Ramadhan, F Mahmood and A Elci. Image denoising by Median filter in wavelet domain. *Int. J. Multimed. Appl.* 2017; **9**, 31-40.
- [13] F Xiaoa and Y Zhang. A comparative study on thresholding methods in wavelet based image denoising. *Adv. Control Eng. Inf. Sci.* 2011; **15**, 3998-4003.
- [14] K Kannan. A new hybrid image denoising algorithm based on Wiener filter and wavelet thresholding. *Int. J. Res. Inf. Technol.* 2017; **1**, 37-45.
- [15] M Longkumer and H Gupta. Denoising of images using wavelet transform, Weiner filter and soft thresholding. *Int. Res. J. Eng. Technol.* 2018; **5**, 231-4.
- [16] L Lin. An effective denoising method for images contaminated with mixed noise based on adaptive Median filtering and wavelet threshold denoising. *J. Inf. Process. Syst.* 2017; **14**, 539-51.
- [17] G Wang, Z Wang and J Liu. A new image denoising method based on adaptive multiscale morphological edge detection. *Math. Probl. Eng.* 2017; **2017**, 1-11.
- [18] H Naimi. Medical image denoising using dual tree complex thresholding wavelet transform and Wiener filter. *J. King Saud Univ. Comput. Inf. Sci.* 2015; **27**, 40-5.
- [19] P Kumar and SK Agarwal. A color image denoising by hybrid filter for mixed noise. *Int. J. Curr. Eng. Technol.* 2015; **5**, 1565-72.
- [20] PM Tayade and SP Bhosale. Medical image denoising and enhancement using DTCWT and Wiener filter. *Int. J. Adv. Res. Ideas Innov. Technol.* 2018; **4**, 342-4.
- [21] J Ho and TL Hwang. Wavelet Bayesian network image denoising. *IEEE Trans. Image Process.* 2013; **22**, 1277-90.
- [22] R Brar and R Kumar. Image denoising using wavelet thresholding hybrid approach. *In: Proceedings of the SARC-IRAJ International Conference, New Delhi, India.* 2013, p. 42-5.
- [23] L Boucher and B Boashash. Wavelet denoising based on the MAP estimation using the BKF prior with application to images and EEG signals. *IEEE Trans. Signal Process.* 2013; **61**, 1880-94.
- [24] M Kaur, K Sharma and N Dhillon. Image denoising using wavelet thresholding. *Int. J. Eng. Comput. Sci.* 2013; **2**, 2932-5.
- [25] J Meenal, S Sharma and RM Sairam. Effect of blur and noise on image denoising based on PDE. *Int. J. Adv. Comput. Res.* 2014; **3**, 236-41.
- [26] V Roy and S Shukla. *Image denoising by data adaptive and non-data adaptive transform domain denoising method using EEG signal.* Springer, India, 2012, p. 1-21.
- [27] P Charde. A review on image denoising using wavelet transform and Median filter over AWGN channel. *Int. J. Technol. Enhanc. Emerg. Eng. Res.* 2013; **1**, 44-7.
- [28] BBS Kumar, PS Satyanarayana, GV Rohini and N Savitha. Edge segmented brain tumor image denoising using wavelets. *Int. J. Appl. Eng. Res.* 2015; **10**, 44.
- [29] S Agrawal and Y Bahendwar. Denoising of MRI images using thresholding techniques through wavelet. *Int. J. Comput. Appl. Eng. Sci.* 2011; **1**, 361-4.
- [30] SD Ruikar and DD Doye. Wavelet based image denoising technique. *Int. J. Adv. Comput. Sci. Appl.* 2011; **2**, 49-53.
- [31] DL Donoho and IM Johnstone. Denoising by soft-thresholding. *IEEE Trans. Inf. Theory* 1995; **41**, 613-27.
- [32] BBS Kumar, PS Satyanarayana and GV Rohini. Image brain tumor edge & watershed segmentation and denoising using DWT. *Int. J. Sci. Eng. Res.* 2014; **5**, 612-20.
- [33] S Garg, R Vijay and S Urooj. Statistical approach to compare image denoising techniques in medical MR images. *Procedia Comput. Sci.* 2019; **152**, 367-74.

- [34] H Hu, B Li and Q Liu. Removing mixture of gaussian and impulse noise by patch-based weighted means. *J. Sci. Comput.* 2014; **67**, 103-29.
- [35] A Aydikia, OY Ismaelb and F Basciftci. Image de-noising using 2-D circular-support wavelet transform. *Am. Sci. Res. J. Eng. Technol. Sci.* 2018; **42**, 1-13.